



Woods, B. K. S., Parsons, L. L., Coles, A. B. N., Fincham, J. H. S., & Friswell, M. I. (2016). Morphing elastically lofted transition for active camber control surfaces. *Aerospace Science and Technology*, 55, 439-448. <https://doi.org/10.1016/j.ast.2016.06.017>

Peer reviewed version

Link to published version (if available):  
[10.1016/j.ast.2016.06.017](https://doi.org/10.1016/j.ast.2016.06.017)

[Link to publication record in Explore Bristol Research](#)  
PDF-document

This is the author accepted manuscript (AAM). The final published version (version of record) is available online via Elsevier at <http://dx.doi.org/10.1016/j.ast.2016.06.017>. Please refer to any applicable terms of use of the publisher.

## University of Bristol - Explore Bristol Research

### General rights

This document is made available in accordance with publisher policies. Please cite only the published version using the reference above. Full terms of use are available:  
<http://www.bristol.ac.uk/red/research-policy/pure/user-guides/ebr-terms/>

# PREPRINT DRAFT

Manuscript accepted for publication in Aerospace Sciences and Technology

## Morphing Elastically Lofted Transition for Active Camber Control Surfaces

**Benjamin K.S. Woods\***

*University of Bristol, Bristol, UK, BS8 1TR*

**Laura Parsons<sup>†</sup>, Alexander B. Coles<sup>‡</sup>, James H.S. Fincham<sup>§</sup>, and Michael I. Friswell<sup>¶</sup>**

*Swansea University, Swansea, UK, SA2 8PP*

### Abstract

This paper introduces a compliant morphing flap transition that seeks to address a long-standing source of noise and drag in the design of aircraft wings – the gap present at the spanwise ends of the control surfaces. These gaps create large discontinuities in the flow and allow for pressure leakage from the lower to upper wing surface, generating significant amounts of vorticity, noise, and drag. The concept introduced here seals this gap with a smooth, three-dimensional morphing transition section that elastically lofts between the rigid wing and moving control surface in a passive and continuous manner. Previous transition concepts are first discussed, followed by establishment of an initial desired transition shape. Computational fluid dynamics analysis of the desired transition shape indicates both an increase in lift and a decrease in drag. The morphing, elastically lofted transition concept proposed here will then be introduced. In this concept, the complex three-dimensional shape change required is created with a novel structural architecture that combines material and geometric compliance with geometric bend-twist coupling. The concept design and operating principles will be introduced, relevant geometric parameters will be derived, and an initial prototype demonstrator capable of large deflections and smooth transition surfaces will be shown.

### Nomenclature

$C_d$  drag coefficient

$C_l$  lift coefficient

\* Lecturer in Aerospace Structures, Dept. of Aerospace Engineering, [ben.k.s.woods@bristol.ac.uk](mailto:ben.k.s.woods@bristol.ac.uk)

<sup>†</sup> Undergraduate Researcher, College of Engineering, [laurapar@ymail.com](mailto:laurapar@ymail.com)

<sup>‡</sup> Undergraduate Researcher, College of Engineering, [alexandercoles@hotmail.co.uk](mailto:alexandercoles@hotmail.co.uk)

<sup>§</sup> Research Officer, College of Engineering, [james@fincham.me.uk](mailto:james@fincham.me.uk)

<sup>¶</sup> Professor of Aerospace Structures, College of Engineering, [m.i.friswell@swansea.ac.uk](mailto:m.i.friswell@swansea.ac.uk)

$c_t$	chordwise length of morphing portion of rib
$h$	half-amplitude of control surface displacement
$l$	spanwise length of morphing portion of transition
$w$	trailing edge displacement
$y$	spanwise distance along transition
$\alpha$	skew angle of corrugations
$\beta$	bend-twist coupling ratio
$\Delta C_l$	change in lift coefficient
$\theta$	rotation angle of trailing edge tip of transition/rib

## Introduction

The gaps present at the ends of aerodynamic control surfaces such as flaps and ailerons are known to be significant sources of noise and drag,[1],[2] and researchers have long sought to build structures capable of bridging these gaps. However, success to date has been elusive as the changes in geometry required are quite significant, the aerodynamic load levels are substantial, and the deformations are fully three-dimensional, making mechanical solutions difficult. Figure 1 shows the wing of an Airbus A380 with multiple control surfaces deflected, and the significant size of the resulting gaps can be seen. The relevance of this problem is increasing as multiple segment control surfaces become more common (creating additional gaps), and as control surfaces are increasingly used not just as control effectors for occasional maneuvers but also to actively and continuously manage the lift distribution of a wing. The impact of these gaps on the drag and noise of the aircraft can be significant. In an industry that is facing increasing pressure to improve operating efficiency throughout the full range of flight conditions and to reduce noise generated, particularly on take-off and landing, a device which can help address both problems and which has potential to be retrofit into existing aircraft is particularly attractive.



Figure 1. Airbus A380 wing with multiple control surfaces deflected showing the large gaps created.[3]

## Background

Work by various industrial and academic research groups has suggested a number of different approaches to sealing these gaps. In 1984, Kunz proposed a mechanical approach with an auxiliary flap perpendicular to the main flap and connected to it with a sliding interface, as seen in Figure 2a.[4] It is not known if this device was ever built, but it would seem to require a significant amount of mechanical complexity. Later, in 1998, Diller and Miller of Northrop Grumman proposed a combined mechanical/compliant transition for the spanwise ends of rigid flaps and as a covering for the chordwise gap at the start of the flap.[5] Shown schematically in Figure 2b, their approach covered the gap between flap and wing with compliant silicone elastomer skins which were mechanically reinforced with a large number of embedded rods. These rods were intended to slide into and out of holes in the silicone rubber to allow for the change in length required of the transition, as seen in Figure 2c. The use of so many sliding interfaces passing through the elastomeric material, which would have a high coefficient of friction and which would be susceptible to wear, is problematic and the concept does not seem to have been adopted. Caton *et al.* of The Boeing Company patented a surprisingly similar concept in 2002,[6] which uses the same approach of reinforcing rods sliding inside of an elastomer skin as shown in Figure 2d. The primary difference between their approach and that of Diller and Miller is use of two shorter reinforcing rods instead of a single longer one. This change requires the inclusion of an additional component to cover the joint (which requires even more sliding interfaces), and the design is still likely to suffer from significant tribological issues. In 2013 a second concept from Boeing, shown in Figure 2e, was patented which creates a smooth outer transition surface by covering a series of rigid, mechanical elements in an elastomeric skin.[7] A number of rigid rib segments are mounted to spanwise rods, which slide into and out of the rigid portion of the wing to create the changing length required of the transition section. Of particular note in this design is the use of rotating tips at the trailing edge extents of each rib. This additional mechanical degree of freedom allows the angle of the trailing edge to rotate to follow the smooth shaped desired. This approach requires, however, that the skin is not attached to the rigid rib sections for a significant chordwise length, which raises concerns about out-of-plane deflection under aerodynamic loading. The rotating tips further increase the number of mechanical joints, adding weight and exacerbating concerns about maintainability.

In 2012, a group from NASA Langley research center patented a compliance based approach to flap transitions.[8] Shown in Figure 2f, this concept consisted of a wedge of elastomer bridging the spanwise gap between flap and wing and is significantly simpler than previous approaches. Various configurations were proposed, including solid elastomer, elastomer skins with hollow center, and elastomer skins over foam core.

This concept was one of several noise reduction measures tested in a recent wind tunnel campaign by NASA,[9] and was shown to reduce measured noise emissions from a deflected flap by 3 dB or more over a wide frequency range, while also improving the lift to drag ratio of the flap (by an unspecified amount). It appears however, that the device tested was a non-straining elastomeric mockup of the desired shape. This is likely due to the difficulty that was experienced with designing a working version of this transition,[10] wherein the very high strain requirements of ~500% led to unacceptably high force requirements and difficulties designing appropriate fixtures. Attempts to reduce these forces by using the hollowed out configuration led to extensive wrinkling of the transition surface.

Successful transonic wind tunnel testing of a related concept as part of the DARPA smart wing program is overviewed by Kudva.[11] This concept didn't employ transition sections *per se*, at least not in the passive sense being discussed here, but created a similar effect from a series of active camber morphing segments along the span which each had two actuation points. These two degrees of freedom allowed each segment to control the amount of camber and the twist angle of the trailing edge independently. As a result, the camber deflections could be smoothly built up along the span with minimized gaps in between segments. Another compliance based approach was introduced by Pankonien and Inman as a further development of a smart material based active camber concept.[12] This morphing transition concept used an elastomeric skin over 3D printed elastomer honeycomb sub-skin to bridge the gap between different active camber modules along the span of a wing. Low speed wind tunnel testing showed the basic efficacy of the approach, although performance under full-scale aerodynamic loading and energy requirements are unknown. Work by da Rocha-Schmidt and Baier investigated an alternative approach based on shear deformation of a reinforced elastomer skin.[13] The reinforcement in this case consists of a woven metal wire mesh, which is able to deform easily in shear without directly straining the wire filaments. This shear deformable skin is placed over a shear deformable cellular core to create a sandwich structure. Work on this recent concept so far has focused on finite element analysis (FEA) and coupon testing of the skin materials.

One of the more promising concepts shown to date is a morphing transition under development by FlexSys Inc., shown in Figure 2g. This concept has been designed to work in concert with a compliant active camber concept known as FlexFoil<sup>TM</sup> that has been under development for some time.[14] The transition has recently completed flight testing on a modified Gulfstream III jet aircraft,[15] but little is known about the operating principle or performance as these authors were unable to find any academic publications or even patents. What can be seen though from the picture in Figure 2g is that while the device does indeed span the gap between

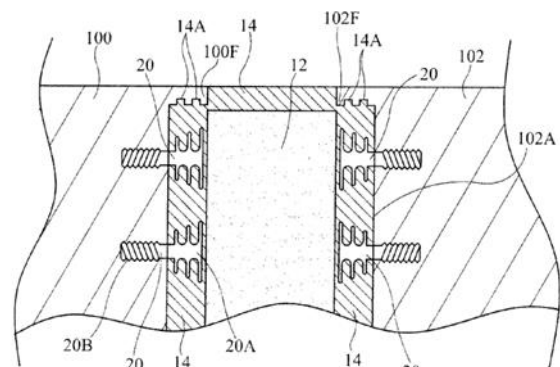
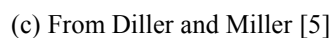
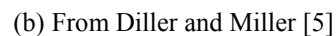
[illegible]

FIG. 4

(e) From Etling [7]

(f) From Khorrami *et al.* [8]



(g) From Lau [15]

Figure 2. A selection of previous flap transition concepts

From this brief review of the existing literature it is clear that engineers have been attempting to solve the problem of flap end gap drag and noise for some time, and that there has been no shortage of ideas. However, much of the work has been carried out by industry and as a result details of the design and performance of these devices is generally unavailable. What's more, with the exception of the newly developed device from FlexSys, none of the proposed solutions appear to have made it to the flight testing stage, and none have been certified for commercial use. It would seem therefore that there is room for the consideration of additional flap end transition concepts.

The previous work shown has been intended for use with a range of control surfaces, including rigid plain flaps, Fowler type flaps, and smooth camber morphing concepts, with the design approach taken in each case and the degrees of freedom achieved determining what types of control surface a given concept is applicable to. The solution proposed here is considered specifically for application to the Fish Bone Active Camber (FishBAC) morphing airfoil, but the basic principles can be readily adapted to other morphing camber concepts. The FishBAC morphing airfoil concept was introduced by Woods and Friswell[16] and has shown promise as a low-drag, high lift authority control surface for application to a wide range of aerodynamic and hydrodynamic surfaces. Wind tunnel testing has shown a 20-25% increase in lift-to-drag ratio at matched lift conditions compared to plain flaps with an achievable change in lift coefficient of  $\Delta C_l > 0.7$ . [17] The smooth continuous change in camber achieved by the FishBAC (as seen in Figure 3) makes it a good candidate for pairing with an end transition device, and the resulting combined surface would have the potential to operate very efficiently. Furthermore, the lack of any external protuberances from the FishBAC (control horns, flap tracks etc.) and the lack of sharp discontinuities in camber change should lead to a low noise solution as well.

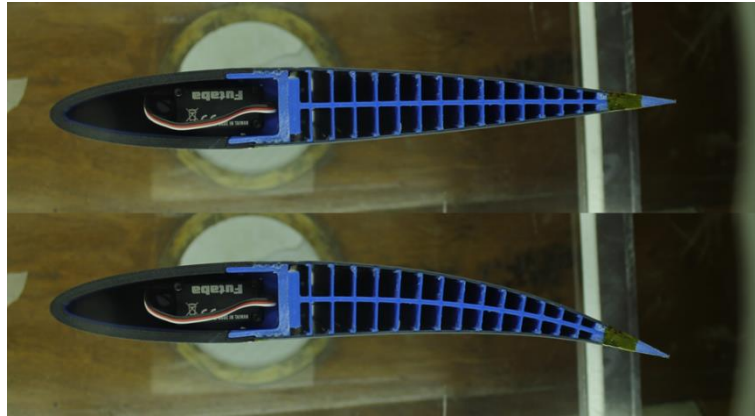


Figure 3. Fish Bone Active Camber morphing airfoil wind tunnel at rest and deflected downwards

## Design Requirements

### *Operating conditions*

The conditions under which this control surface transition must operate are demanding aerodynamically, structurally, and environmentally. Ideally, the transition would be usable on a wide range of vehicles, so operating Mach numbers up to the transonic range may be encountered, although the placement of the transition on the relatively lightly loaded trailing edge does reduce the actual aerodynamic pressures the device must support. Furthermore, the aerodynamic loading will vary considerably, increasing significantly with larger control surface deflections. Since all of the shape change in this transition occurs through compliance, the device must undergo significant direct strain; the skin surface in particular will experience large magnitude strains in multiple directions due to chordwise bending and spanwise elongation, on the order of 10%. Creating a structure which can achieve these large strains under the large aerodynamic loadings with minimal actuation requirements and with suitable levels of fatigue life is challenging. What's more, it must work over a wide range of temperatures, on the order of  $-40^{\circ}\text{C}$  to  $+90^{\circ}\text{C}$  for civil applications and  $-55^{\circ}\text{C}$  to  $+100^{\circ}\text{C}$  for military applications while being exposed to a host of environmental factors including ultraviolet light, exposure to petroleum products and solvents, ice accumulation, and rain and sand erosion. These environmental factors can be particularly difficult for the types of elastomeric materials typically used for high strain applications. Work with elastomeric erosion barriers[18][19] has led to the development of high performance elastomeric materials which have been flight certified, implying that while a challenging part of the problem, there is reason to believe that material solutions can be found. Having established the demanding operating conditions these devices must operate in, we will now consider the difficulties associated with the design process.

### *Design Approach*



The starting point for the design of a morphing transition such as this is not entirely apparent. The primary reason for having the device is aerodynamic, and so the aerodynamic shapes required to minimize the amount of drag and noise generated at the flap ends would seem to be the obvious starting point. However, it is quite difficult to know what the “best” possible shape is for such a device, particularly at the early stages in the development of a new concept. It is expected that the “optimal” shape for any given application would be sensitive to the particulars of the wing it was being installed on and the operating conditions under which it would be used, with Mach number and Reynolds number being two particularly important parameters that would be expected to impact the fluid flow over and around the device. Given the highly three-dimensional nature of the structure and the expected flow around it, and the importance of viscosity effects and flow separation at the trailing edge of the wing, a full understanding of the flow fields around the transition would require a considerable amount of high-fidelity computational fluid dynamics (CFD) analysis. To then optimize the shape using these tools to analyse a large number of potential geometries under a number of different operating conditions is clearly a significant endeavour. What’s more, a reasonable amount of wind tunnel validation of the CFD would be required to establish the validity of the methods, further growing the scope of the problem.

In fact, the high-fidelity optimized shape approach mentioned above, as significant of an effort as it would be, would ultimately not be particularly useful for the case of this device as the compliant nature of the solution proposed implies that the shapes under loading are not the same as the unloaded geometries, and therefore any CFD results which use prescribed, “rigid” shapes would likely deviate significantly from what would exist in flight. Instead, a coupled fluid-structure interaction analysis is needed that can consider the interplay between the compliant structure and the flow field to find stable converged solutions. This of course requires a detailed understanding of the structure and its stiffness properties, which at the start of the design process simply does not exist.

This fundamental design problem exists with all morphing aircraft structures, and indeed increasingly it exists with conventional aerospace structures as well as designers are getting ever more comfortable with larger elastic deflections in wing structures, for example. However, we wish to avoid the full depth of this problem initially to allow us to make some meaningful progress quickly with the new structural architecture proposed. For the sake of this initial development work we will therefore assume some general requirements for the types of shapes obtainable by the structure, and we will design the concept such that there is sufficient control over the design parameters to allow for a number of different desired shapes to be created. If these initial efforts prove

successful, there will then be significantly more information on the behavior of the structure available for future fluid-structure interaction analysis.

### *Nominal Deformed Shapes*

With this in mind, we will establish for our purposes here the very simple aerodynamic design guideline that the deformed shape should be smooth and continuous with no discrete changes in shape. This will minimize discontinuities in the surface which would likely create undesirable aerodynamic flow phenomena such as boundary layer tripping, vortex shedding, interference drag, etc. Furthermore, the two fixed sides of the transition, namely the spanwise edge which attaches to the trailing edge of the wing and the chordwise edge which attaches to the rigid portion of the wing trailing edge should have surfaces which remain tangent to the neighboring wing components across the entire deflection range. The same is true for the moving edge of the transition which attaches to the control surface. Enforcing tangency at all attached edges of the transition will ensure that the resulting combined wing surface is also smooth and continuous.

To further simplify the definition of the desired shape for this initial study, we can focus on the profile of the trailing edge of the morphing transition, with the underlying assumption that if the trailing edge is smooth then the continuous compliance of the rest of the structure will help ensure smoothness elsewhere. We will consider the two-dimensional projection of the trailing edge onto a plane aligned with the spanwise and thickness-wise directions, ignoring for the time being the small amount of motion of the trailing edge in the chord direction and considering just its vertical (thickness-wise) displacement. There are a number of shape functions which could be used to describe the desired deflection of the trailing edge along the span of the device, but one particularly simple and useful one is the cosine function:

$$w(y) = h * \cos\left(\frac{\pi y}{l}\right) - h \quad (1)$$

where  $w$  is the vertical (thickness direction) displacement of the trailing edge,  $y$  is the spanwise distance along the transition,  $h$  is the half-amplitude of the control surface deflection, and  $l$  is the spanwise length of the morphing portion of the transition. Figure 4 shows an example of trailing edge shapes for the case of a nominal transition that is 200 mm long in span, and has an active chordwise length of 200 mm that undergoes a series of control surface deflections from -60 mm to 60 mm ( $h = -30$  to 30 mm). Note that the sign convention used for the shape function follows that used for trailing edge flaps: positive values of  $h$  produce downwards deflections, increasing local camber. It can be seen that this shape function creates a smooth continuous transition between the rigid portion of the trailing edge (left side of the figure) and the morphing control surface (right side) over a

wide range of control surface deflections, both upwards and downwards. This bidirectional capability is important for applications such as ailerons where both positive and negative deflections are required. We will consider these desired shapes further and their impact on the structural design in more detail below, but first we will use these nominal deflected shapes in some initial computational fluid dynamics analysis to establish the potential for drag reduction through use of the morphing transition.

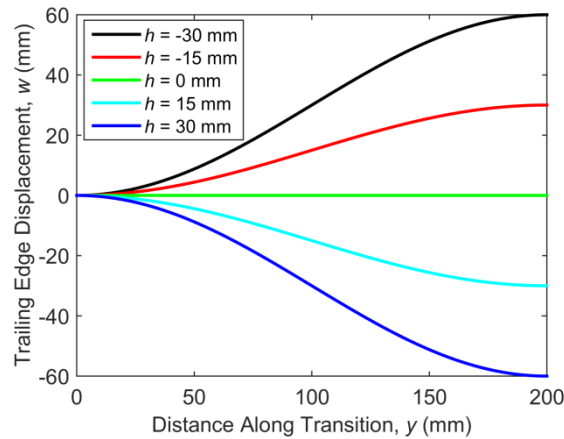


Figure 4. Example desired trailing edge shapes for the morphing transition

### Aerodynamic Analysis of Desired Transition Shapes

A computational fluid dynamics (CFD) study of the proposed morphing transition shape was undertaken using the OpenFOAM software package. The intention of this study was to get some initial idea of the impact on aerodynamic performance (lift and drag) that a transition of the shape proposed here would have. A simple rectangular planform half-wing geometry with a half-span of 10 m, a chord of 1 m and a NACA 0012 airfoil was chosen as a generic geometry with relevance to unmanned aerial vehicles, wind turbines, and helicopter rotors. The operating Reynolds number was  $2.96 \times 10^6$ , corresponding to a freestream velocity  $V_\infty = 87$  m/s, and in all cases the wing was at an angle of attack (defined by the non-morphing portion of the wing) of  $2.5^\circ$ .

A FishBAC morphing control surface is installed in the center of the wing span, with a chordwise length of 25% chord. Due to the spanwise symmetry of the chosen geometry, a half model was studied with a plane of symmetry established in the center of the control surface. The wing shapes analyzed can be seen in Figure 5. For the no transition models (e.g. Figure 5a), the control surface has a span wise length of 2.5 m and the fixed, non-morphing portion of the wing also has a length of 2.5 m. For the control surfaces with end transition (Figure 5b), the spanwise length required for the transition comes equally from the control surface and the fixed portion of the wing, resulting in 2 m fixed span, 1 m transition span, and 2 m FishBAC span.

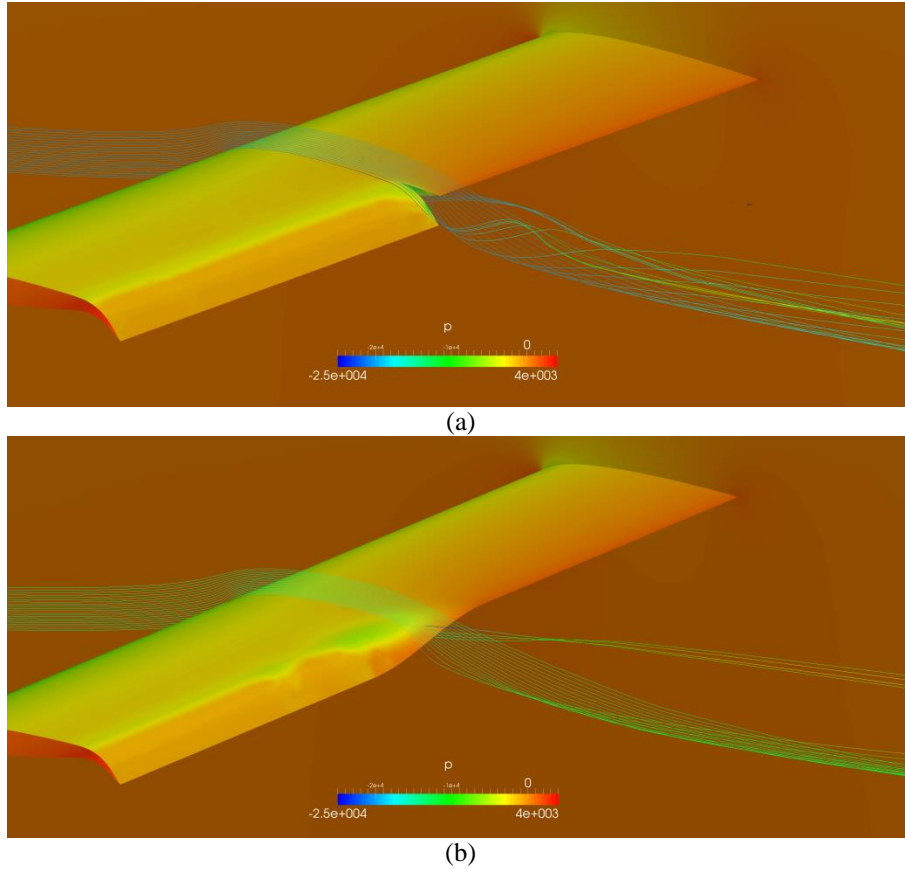


Figure 5. Surface pressure plots with streamlines from OpenFOAM CFD analysis a). no transition and b). with transition

Multiple FishBAC deflections were tested, with trailing edge deflections ranging from 0% – 15% of chord. Based on previous studies,[20] a third-order polynomial was used to describe the chordwise distribution of camber generated from the FishBAC deflections, with the NACA 0012 thickness distribution mapped onto that camber line in a direction perpendicular to the local tangent line, in the standard manner of NACA four digit series airfoils.[21] For the transition, Equation 1 was used to generate the distribution of trailing edge deflections, with the chordwise distribution of camber being described by the same shape function as used for the FishBAC, with the magnitude scaled to hit the desired maximum trailing edge displacement. The models were meshed with the snappyHexMesh software with roughly 10 million cells. The Reynolds-Averaged Navier-Stokes equations were solved by OpenFOAM with the Menter's SST turbulence model.

Initial insight into the need for a transition can be seen in Figure 5a, where streamlines in the CFD results for the wing without transition show a strong vortex formed at the junction between control surface and rigid wing. While rotation of the streamlines is not completely eliminated with the transition, it can be seen in Figure 5b that the downstream rollup of the vortex is no longer present. This reduction in vorticity formation is reflected in the aerodynamic performance of the particular geometries shown in Figure 5 (FishBAC deflection =

15% of chord). The lift and drag coefficients ( $C_L$  and  $C_D$ ) for these cases are tabulated in Table 1 along with the resulting lift-to-drag ratios. Note that the transition both increases lift and decreases drag, leading to an over 7% increase in net lift-to-drag ratio. For the case of no FishBAC deflection there was no difference in performance with the transition (as the wing is essentially a rigid rectangular wing in that case), and as expected the benefits of the transition increase as the FishBAC deflection, and therefore the end gap size, increases.

Table 1. CFD results showing impact of transition for 15% chord FishBAC deflection

	No Transition	Transition	Difference
$C_L$	1.0409	1.0833	+4.07%
$C_D$	0.064	0.062	-3.13%
$C_L/C_D$	16.28	17.46	+7.25%

As this analysis used rigid, prescribed geometries which did not include the effects of compliance, the results shown are not able to provide a full understanding of this highly coupled aero-elastic problem, but as an initial simplified analysis they do help motivate this research by showing the large levels of vorticity generated by the end gap and by providing an indication of the aerodynamic performance improvements possible with sealing it. With these benefits in mind, the novel transition concept proposed here will be introduced.

## Proposed Solution

To address the demanding design requirements of control surface end transitions, a novel structural architecture is proposed here. This Morphing, Elastically Lofted (MELD) transition combines material and geometric compliance with bend-twist coupling to create a structure capable of large three-dimensional deformations that automatically creates the desired combination of bending and twisting along the span needed to create a smooth and continuous aerodynamic surface.[22] The resulting structure is therefore elastically lofted between the control surface and rigid wing structure in a continuous, passive manner, melding the two structures together. The MELD transition, which is shown schematically Figure 6, is based around a series of bend-twist coupled ribs which are stacked along the span of the module and which are held together by a frame which mounts to the trailing edge of the rigid portion of the wing. The amount of bend-twist coupling in each of the ribs is carefully tailored to achieve the desired distribution of trailing edge angle along the span. At the spanwise extents of the transition there are separate end ribs which are designed to be easily attached to the existing wing structure. One of these ends is rigid, and the other has the camber morphing geometry of the FishBAC (or similar) active camber control surface to which it attaches. The bend-twist coupled ribs, mounting frame, and end ribs are all covered with an elastomeric skin made of silicone or polyurethane rubber sheets,

which may or may not be reinforced selectively with fiber, and which are bonded to the upper and lower surfaces. Taken together, these components create a MELD module that can be installed and removed relatively easily into a wing structure, has no mechanical moving parts, and which requires no dedicated actuation; as it is passively driven by the control surface. These features are intended to simplify integration of the transition into new wing designs, and to open up the possibility of retrofitting it into existing designs alongside a retrofit of the FishBAC camber morphing airfoil, which can also be designed as an independent module for ease of integration.

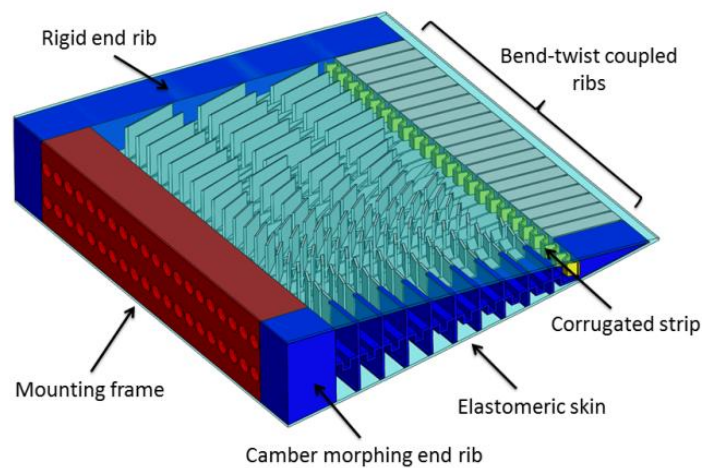


Figure 6. MELD transition concept

### *Geometric Bend-twist Coupling with Skewed Corrugations*

The bend-twist coupled ribs are the key enabling technology for this transition, so their design and operating principle will be discussed in detail here. Driven by the need for high levels of coupling between elastic bending and twisting, the rib sections in this concept use what is believed to be a novel compliant morphing approach that links the two deformations using skewed corrugations. Corrugations are well known in morphing structures and have been proposed in a variety of configurations, albeit most often as an anisotropic extensible skin surface.[23] Corrugated structures have highly direction dependent stiffness, with the direction perpendicular to the corrugations being significantly stiffer in extension and in bending than the direction along the corrugations. Due to their highly anisotropic nature, corrugations are an effective way to create a compliant structure which deforms primarily in one direction. The corrugations in essence act like a series of compliant hinges, allowing for bending deformations to be built up as a series of small deformations in these hinges, which is realized physically as thin plate bending of the segments of the corrugation.

Corrugated members can form the basis of camber morphing ribs, as the corrugated geometry allows for chordwise bending while retaining stiffness in the other loading directions. Figure 7 shows an airfoil trailing edge rib structure built around a corrugated spine.

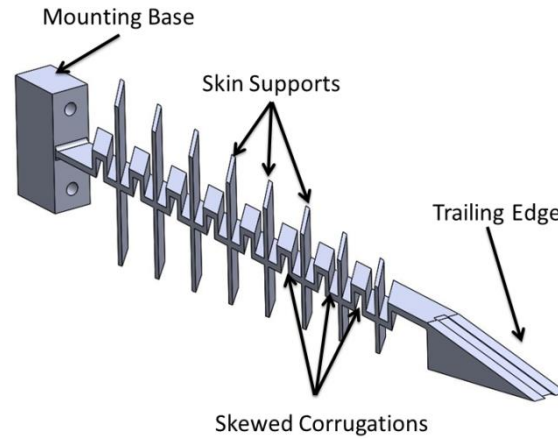


Figure 7. Bend-twist coupled rib with skewed corrugations

If the direction of the corrugation is aligned with the length axis of a rib structure, then the bending of the corrugation will lead to pure bending of the rib, with no induced rotation. If, however, the corrugation is placed at an angle  $\alpha$  which is skewed to the long axis of the rib, as in Figure 8, then the bending of the corrugation members will induce twisting in the rib. This is a geometrically induced coupling which unlike other bend-twist coupling concepts does not require asymmetric or unbalanced composite layups or material anisotropy to work.[24][25][26] Composites are indeed preferred materials for the MELD transition as they can provide excellent stiffness and strength properties with low mass, but the concept is not predicated on their use. In addition to allowing for a greater range of materials to be used, the skewed corrugations are also capable of realizing particularly high levels of bend-twist coupling. This is demonstrated in Figure 9 with the finite element analysis results of a skewed corrugation rib under tip load. In this study the mounting base is fixed while the rest of the structure is free to deform under the applied vertical tip load  $P$ . The deformed shape shown in Figure 9 is shown at a scale of unity, and the large tip rotation which the tip load induces is clearly visible and is the direct result of the use of skewed corrugations. Having introduced the manner in which bend-twist coupling is created in the MELD transition, we will now consider the required distribution of coupling along the span of the transition.

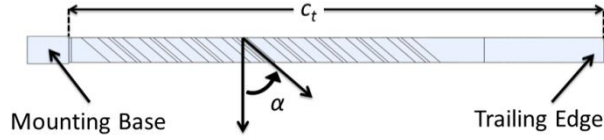


Figure 8. Bend-twist coupled rib, top view showing definition of skew angle  $\alpha$

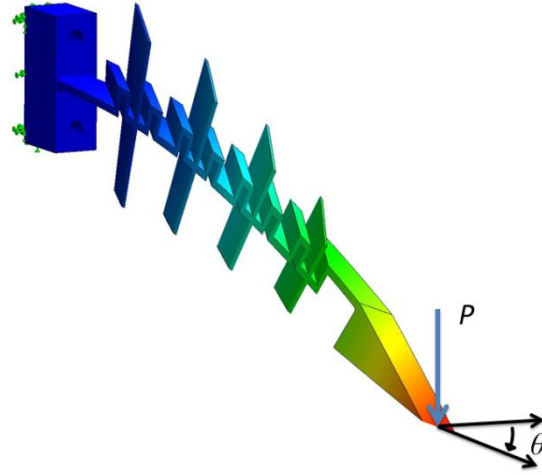


Figure 9. Finite element analysis result of a skewed corrugation rib ( $\alpha = 69^\circ$ ) under tip load  $P$  – note rotation of trailing edge tip relative to the mounting base by angle  $\theta$

### *Bend-Twist Coupling Requirements to Achieve Nominal Shapes*

One of the core features of the MELD concept is the ability of the ribs to match both the desired displacement and local surface angle over a range of control surface deflections. The local trailing edge tip angle  $\theta$  that must be achieved at each point along the span can be found by differentiating the desired deflection:

$$\theta(y) = w'(y) = -\frac{\pi h}{l} \sin\left(\frac{\pi y}{l}\right) \quad (2)$$

For the example trailing edge shapes shown in Figure 4, the corresponding trailing edge angles are shown in Figure 10.

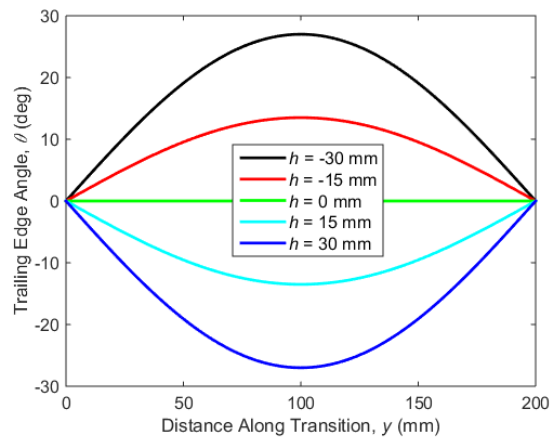




Figure 10. Distribution of trailing edge angle for the desired shapes

We can now define a geometric bend-twist coupling parameter,  $\beta$ , which determines the ratio of rotation to deflection that the tip of each rib must achieve:

$$\beta(y) = \frac{\theta/c_t}{w/c_t^3} = \frac{\theta}{w} c_t^2 \quad (3)$$

The tip angle and deflection are both normalized using the length of the compliant portion of the rib  $c_t$ , which is shown in Figure 8, to make  $\beta$  a more generally comparable term that is less beholden to the specifics of the transition geometry. The tip deflection is normalized by  $c_t$  to the third power to reflect the distribution of deflection expected under a tip load according to linear elastic beam bending theory (for constant flexural rigidity) and the tip rotation angle is similarly normalized linearly by  $c_t$  in line with linear elastic torsional beam theory.[27]

For the example trailing edge shape given in Equation 1, we can evaluate Equation 3 to give the required distribution of bend-twist coupling for the desired shape:

$$\beta(y) = \frac{-\frac{\pi h}{l} \sin(\frac{\pi y}{l})}{h \cos(\frac{\pi y}{l}) - h} c_t^2 = \frac{\pi c_t^2}{l} \cot \frac{\pi y}{2l} \quad (4)$$

which is plotted in Figure 11. It is interesting to note that the half amplitude,  $h$  drops out of the equation, such that the distribution of coupling required is independent of both sign and amplitude of the desired deflection. This is ideal of course as the control surface to which the MELD transition is attached would be expected to work over a range of upwards and downwards deflections and the value of  $\beta$  of a given rib is an intrinsic geometric property that cannot be changed once manufactured. Note also that the cotangent function approaches infinity at  $y = 0$ , so the vertical axis of Figure 11 has been truncated to show the primary region of interest.

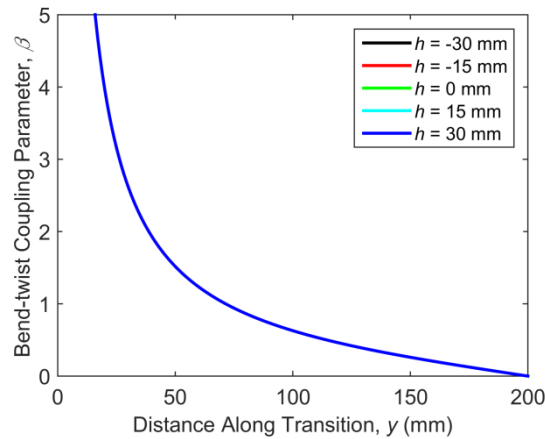


Figure 11. Distribution of bend-twist parameter required to obtain the desired trailing edge shapes – all lines are coincident

The relationship between the values of corrugation skew angle and bend-twist parameter for a given rib is governed by the manner in which the skewed corrugations induce coupling, which in turn is dependent on the detailed geometry and material properties of that rib. For this initial study, a series of ribs with varying skew angle (but equivalent geometry otherwise) were studied using the SolidWorks Simulation finite element analysis program to determine the impact that skew angle  $\alpha$  had on the resulting bend-twist parameter  $\beta$  for that specific rib geometry. Both the tip deformation and rotation angle varied linearly with applied load for a wide range of loads, such that a single value of  $\beta$  could be ascribed for a given rib over the full range of deflections of interest for this study. The details of the rib geometry used for the initial demonstrator are discussed in the Concept Demonstrator section. The results of this FEA study are shown in Figure 12. It was found that a simple empirically fit tangent function:

$$\beta = A \tan(\alpha) \quad (5)$$

captured the relationship between  $\beta$  and  $\alpha$  quite well when  $A = 0.28$ , which is plotted along with the FEA data in Figure 12. Note that while  $\alpha$  is plotted in degrees, Equation 5 is evaluated in radians.

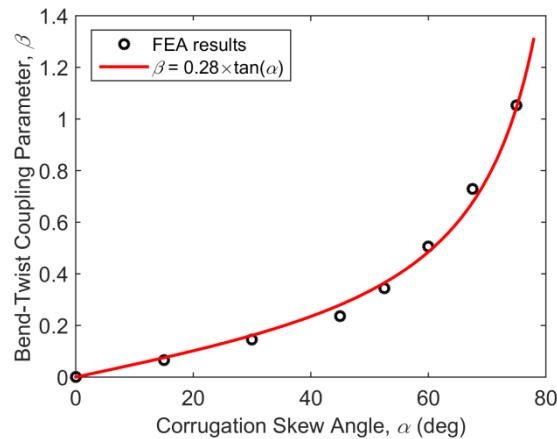


Figure 12. Results from finite element analysis of ribs with an empirically fit tangent function showing the relationship between bend-twist coupling and skew angle for the specified rib geometry

By combining Equation 5 and Equation 4 we can solve for the distribution of skew angle along the span required to achieve the distribution of bend-twist coupling shown in Figure 11. While the required bend-twist coupling value approaches infinity as  $y$  approaches 0, the corresponding values of skew angle approach a finite value of  $\alpha = 90^\circ$ , as can be seen in Figure 13. This is due to the tangent function approaching infinity at  $90^\circ$ . However, it is not feasible to make skewed corrugated ribs with angles that high, as the chordwise length required for even a single segment of corrugation at values of  $\alpha$  approaching  $90^\circ$  quickly exceeds the space available. Design work and 3D printing of specimens has shown a maximum practically achievable skew angle of roughly  $\alpha = 75^\circ$  for the ribs used here. This restraint is reflected in Figure 13 by the dashed line. The

saturation of the skew angle implies that the initial portion of the transition (on the end closest to the rigid portion of the wing) would not have quite as much coupling as desired. However, while the desired coupling is high, the actual deformations and rotations required are quite low, implying that any errors in shape would be small relative to the overall size of the device. The impact of the skew angle saturation is further mitigated by the compliant connections which exist between the ribs which help smooth the shape, as discussed in the next section.

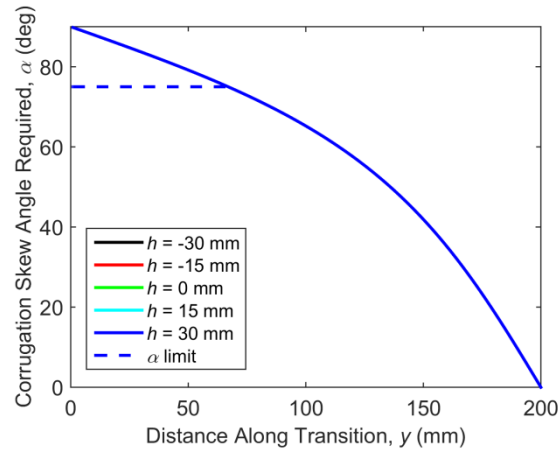


Figure 13. Distribution of required skew angle along span – all values of  $h$  are coincident

### *Connections between Rib Members*

While the skew corrugated rib members are designed to automatically obtain the desired twist angle when bent, they still require a means of applying the required bending forces. This is accomplished in two ways in the present concept; through the skin and through supplementary corrugated strips. The elastomeric skin which covers the upper and lower surfaces of the MELD transition acts as a compliant connection between adjacent rib members. As it is bonded to both the fixed and moving ends of the control surface, when the control surface is deflected the skin will be directly stretched. Since the skin is also bonded to the ribs, it will to a certain extent bend the ribs along with it, and has some ability to apply force to the ribs. However, in cases where the skin is able to be designed to be quite soft (for lower dynamic pressures for example) or where the ribs are required to be particularly stiff, it is likely that the skin alone will not be able to ensure that sufficient force is applied to the ribs to create the required distribution of bending, leading to discontinuities in the deformed shape. To address this, the MELD concept includes thin spanwise corrugated strips that connect the ribs to the rigid and flexible ends of the transition. The number and location of these connection members is an open design variable which is expected to change for different operating conditions and geometries. For this work a single corrugated strip is included near the trailing edge, as visible in Figure 6. The geometry and orientation of this component allows

it to stretch, bend and rotate as required to undergo the deformation required at the trailing edge while allowing for the transfer of force between rib members. A wide range of stiffness properties and actuation energy requirements are achievable through varying the geometry, material properties, number, and chordwise location of the corrugated rib connection members, allowing the MELD transition to be adapted to a wide range of applications and operating conditions.

## **Concept Demonstrator**

To show the structural viability of the MELD transition concept, an initial prototype demonstrator has been designed and built. This demonstrator, the design model of which is shown in Figure 6, was sized for use with a 33% chord FishBAC (i.e. morphing starts at 67% chord) on a 600 mm chord wing section with a NACA 0012 profile. This gives the morphing portion of the demonstrator a chordwise length of 200 mm, with an additional 30 mm of chordwise length included for the non-morphing mounting frame and to provide a bonding surface for the elastomeric skin. The total spanwise length of the demonstrator is 250 mm, with the bend-twist coupled ribs totaling 200 mm and the fixed and morphing end ribs each spanning 25 mm. While these geometry parameters are nominal, they are meant to be representative of a range of wing structures useful for manned and unmanned aircraft, helicopter blades, and wind turbine blade applications. A total of twenty skewed corrugation ribs, each a nominal 10 mm wide, are spaced between the end ribs with corrugation skew angles ranging from  $5.06^\circ$  to  $75^\circ$ . The value of  $\alpha$  for each rib was taken from Figure 13, with the value corresponding to the spanwise center point of each rib being used. Extensions are included off of the corrugated portion of each rib that follow the airfoil contour to provide bonding pads for the silicone skin. The skewed corrugations and skin bonding extensions generally extend to within 60 mm of the trailing edge, although this value varies slightly with skew angle. The bend-twist coupling feature does not extend all the way to the trailing edge due to the limited space available in the sharp trailing edge, and due to the desire to have a rigid region at the end of the rib to create sufficient area to bond the skin to. A single corrugated rib connection member mounted 50 mm in from the trailing edge connects the end ribs to the bend-twist coupled ribs.

This model took advantage of additive manufacturing technology to simplify fabrication of the components, as the combination of skewed corrugations and airfoil profile shaped projections makes for an admittedly complex geometry which would be challenging to make using traditional metal or composite manufacturing methods. While the entire model could have been printed as a single monolithic part, as a means of risk reduction and to allow some ability to replace and change components, the ribs and support pieces were all

printed individually. An HP DesignJet 3D Fused Deposition Modeling (FDM) printer was used to print the components in ABS plastic.

The silicone skin consists of two separate 1.5 mm thick silicone sheets pre-tensioned and bonded to the structure. Pre-tensioning increases out-of-plane bending stiffness of the skin allowing it to better resist aerodynamic loading, and eliminates buckling of the skin surface in areas which undergo compressive strains upon deformation. This approach is adopted directly from previous analytical and experimental work on the FishBAC, which has shown it to be an effective means of reducing undesired deformations in the compliant skin.

The assembled demonstrator is shown in Figure 14 cantilevered from its mounting frame. This MELD transition behaves as desired, exhibiting smooth and continuous surface shapes when deformed. The importance of the bend-twist coupling to the operation of the device can be seen by the behavior of the portion of the device over which it does not exist. As mentioned above, due to the thinness of the trailing edge, the skewed corrugations stop roughly 60 mm from the trailing edge. The lack of bending compliance and bend-twist coupling in this region leads to the formation of small stepped discontinuities, as can be faintly seen in Figure 14 at the very end of the trailing edge. This effect is small though and can likely be addressed in future designs with geometry changes and/or an additional rib connection member closer to the trailing edge. The lack of any such stepped shape over the rest of the MELD transition demonstrator as it elastically lofts between a prescribed 60 mm tip deflection at the morphing end and no deflection at the fixed end proves the efficacy of the compliant, bend-twist coupled design architecture. Although not shown in the figure, this demonstrator is fully capable of bidirectional deflections as desired.



Figure 14. MELD transition demonstrator as built: a) at rest and b) deforming due to tip load applied to camber morphing end

While the ability of the demonstrator to achieve the desired smoothness in its deformed shape is encouraging, there is clearly more work required to establish the viability of the MELD transition concept. To this end, structural characterization of the demonstrator is ongoing in parallel to finite element analysis of the entire structure. From there, high fidelity modeling of the aerodynamic performance will need to be validated against wind tunnel data, and this coupled fluid-structure interaction problem will need to be solved in a manner which allows for optimization of the design of the MELD transition both aerodynamically and structurally.

## **Conclusions**

In conclusion, this work has introduced a new morphing structure designed to seal the large gaps created at the end of a morphing camber control surface when it is used. These spanwise end gaps are a significant source of drag and noise in current aircraft, and there has been a lot of interest both historically and recently in the design of structures capable of sealing them. Here, a Morphing Elastically Lofted (MELD) transition was proposed which combines material and geometric compliance with bend-twist coupling to create a unique structural architecture capable of deforming in a smooth and continuous manner to connect the moving end of an active camber morphing control surface to the fixed wing structure around it. The inclusion of bend-twist coupling allows the structure to automatically deform in a manner which allows for both the desired local surface displacements and angles to be achieved. Existing work in this area was first introduced, followed by an overview of the design requirements for end transitions. The difficulty of analyzing these structures, particularly for initial design work, due to the strong coupling between aerodynamics and structural deflections and the highly three dimensional nature of the problem was highlighted. This led to the establishment of a nominal target shape as a starting point, which was shown to provide improved aerodynamic performance in an initial CFD study. The operating principles of the proposed MELD transition were then introduced, with particular attention paid to the design of the skewed corrugation features used in the rib sections as a geometric means of creating the desired bend-twist coupling. The distributions of trailing edge angle and bend-twist coupling required to achieve the target shape were then derived, and a finite element analysis study provided the relationship between corrugation skew angle and bend-twist coupling parameter for the proposed geometry, thereby allowing for the distribution of corrugation skew angle along the span to be determined. An initial technology demonstrator was built with this calculated geometry, and was shown to deform in the desired manner, creating a smooth, elastically lofted shape with minimal surface discontinuities. The basic operating principle of the MELD concept has therefore been demonstrated and the usefulness of the bend-twist coupling

shown, although much work remains to be done to develop appropriate analysis tools and to show the efficacy of the concept in realistic operating environments.

## Acknowledgements

This work was funded in part under the European Research Council under the European Union's Seventh Framework Programme (FP/2007-2013) / ERC Grant Agreement n. [247045].

## References

- [1] M. G. Macaraeg, "Fundamental Investigations of Airframe Noise," NASA Langley Research Center, Hampton, VA, USA, Technical Report 20040090482, Jan. 2004.
- [2] U. Michel, J. Helbig, B. Barsikow, M. Hellmig, and M. Schuettpelz, "Flyover noise measurements on landing aircraft with a microphone array," in *4th AIAA/CEAS Aeroacoustics Conference*, Toulouse, France, 1998.
- [3] Aviation Stack Exchange, "Why do some aircraft have multiple ailerons per wing? - Aviation Stack Exchange," 28-Aug-2015. [Online]. Available: <http://aviation.stackexchange.com/questions/921/why-do-some-aircraft-have-multiple-aileron-per-wing>. [Accessed: 06-Aug-2015].
- [4] R. Kunz, "Apparatus for closing an air gap between a flap and an aircraft. US Patent No. US4471925A. Issued Sep 18, 1984," US4471925 A, 18-Sep-1984.
- [5] J. B. Diller and N. F. Miller, "Elastomeric transition for aircraft control surface. US Patent No. US6145791A. Issued Nov. 14, 2000," US6145791 A, 14-Nov-2000.
- [6] J. H. Caton, M. J. Hobey, J. D. Groeneveld, J. H. Jacobs, R. H. Wille, and L. O. B. Jr, "Control surface for an aircraft. US Patent No. US6349903B2. Issued Feb. 26, 2002," US6349903 B2, 26-Feb-2002.
- [7] K. A. Etling, "Morphing control surface transition. US Patent No. US8342447B2. Issued Jan. 1, 2013," US8342447 B2, 01-Jan-2013.
- [8] M. R. Khorrami, D. P. Lockard, J. B. Moore, J. Su, T. L. Turner, J. C. Lin, K. M. Taminger, S. K. Kahng, and S. A. Verden, "Elastically deformable side-edge link for trailing-edge flap aeroacoustic noise reduction. US Patent No. US8695925B2. Issued Apr. 15, 2014," US8695925 B2, 15-Apr-2014.
- [9] M. R. Khorrami, W. M. Humphreys, D. P. Lockard, and P. A. Ravetta, "Aeroacoustic Evaluation of Flap and Landing Gear Noise Reduction Concepts," presented at the AIAA Aviation and Aeronautics Forum and Exposition, Atlanta, GA, United States, 2014.
- [10] T. Sreekantamurthy, T. L. Turner, J. B. Moore, and J. Su, "Elastomeric Structural Attachment Concepts for Aircraft Flap Noise Reduction - Challenges and Approaches to Hyperelastic Structural Modeling and Analysis," in *55th AIAA/ASME/ASCE/AHS/SC Structures, Structural Dynamics, and Materials Conference*, National Harbor, Maryland, USA, 2014.
- [11] J. N. Kudva, "Overview of the DARPA Smart Wing Project," *J. Intell. Mater. Syst. Struct.*, vol. 15, no. 4, pp. 261–267, Apr. 2004.
- [12] A. Pankonien and D. J. Inman, "Experimental testing of spanwise morphing trailing edge concept," in *Proceedings of SPIE*, 2013, vol. 8688, pp. 868815–868815–13.
- [13] L. da Rocha-Schmidt and H. Baier, "A Shape Variable Gap Cover Concept for Aerodynamic Control Surfaces Based on Shear Deformation," in *63. Deutscher Luft- und Raumfahrtkongress*, 2014.
- [14] J. Hetrick, R. Osborn, S. Kota, P. Flick, and D. Paul, "Flight Testing of Mission Adaptive Compliant Wing," in *48th AIAA/ASME/ASCE/AHS/ASC Structures, Structural Dynamics, and Materials Conference*, Honolulu, Hawaii, 2007.
- [15] S. Lau, "Wing morphing experiment takes flight," *Professional Pilot Magazine*, Apr-2015.
- [16] B. K. S. Woods and M. I. Friswell, "Preliminary Investigation of a Fishbone Active Camber Concept," in *Proceedings of the ASME 2012 Conference on Smart Materials, Adaptive Structures and Intelligent Systems*, Stone Mountain, GA, 2012, pp. 555–563.
- [17] B. K. S. Woods, O. Bilgen, and M. I. Friswell, "Wind tunnel testing of the Fish Bone Active Camber morphing concept," *J. Intell. Mater. Syst. Struct.*, vol. 25, no. 7, Feb. 2014.
- [18] R. L. Kreitingner and D. B. Middleton, "Aircraft Surface Coatings for Drag Reduction/Erosion Protection," SAE International, Warrendale, PA, SAE Technical Paper 811070, Oct. 1981.
- [19] W. . Wright, "Polymers in aerospace applications," *Mater. Des.*, vol. 12, no. 4, pp. 222–227, Aug. 1991.

- [20] B. K. S. Woods, I. Dayyani, and M. I. Friswell, "Fluid-Structure Interaction Analysis of the Fish Bone Active Camber Morphing Concept," *J. Aircr.*, vol. 52, no. 1, pp. 307–319, 2015.
- [21] I. H. Abbott and A. E. V. Doenhoff, *Theory of Wing Sections, Including a Summary of Airfoil Data*. New York, New York: Dover Publications Inc., 1959.
- [22] B. K. S. Woods, M. Friswell, and L. Parsons, "Morphable Structure," GB1412159.4, 08-Jul-2014.
- [23] C. Thill, J. A. Etches, I. P. Bond, K. D. Potter, and P. M. Weaver, "Composite corrugated structures for morphing wing skin applications," *Smart Mater. Struct.*, vol. 19, no. 12, p. 124009, Dec. 2010.
- [24] R. M. Jones, *Mechanics of Composite Materials*, Second Edition. Philadelphia, PA: Taylor and Francis, Inc, 1999.
- [25] R. Chandra and I. Chopra, "Experimental and theoretical analysis of composite I-beams with elastic couplings," *AIAA J.*, vol. 29, no. 12, pp. 2197–2206, 1991.
- [26] Don Lobitz and Paul Veers, "Aeroelastic behavior of twist-coupled HAWT blades," in *1998 ASME Wind Energy Symposium*, Reno, Nevada, 1998.
- [27] L. Meirovitch, *Fundamentals of Vibrations*. New York, NY: McGraw Hill, 2010.